ROBUST DESIGN OPTIMIZATION OF RETAINING WALL BACKFILLED WITH SHREDDED TIRE IN THE FACE OF EARTHQUAKE HAZARDS

Nadarajah Ravichandran[a], Lei Wang[b*], Parishad Rahbari[c], C. Hsein Juang[d]

[a]Associate Professor, Glenn Department of Civil Engineering, Clemson University, Clemson, SC 29634, United States, E-mail: nravic@clemson.edu
[b]Assistant Professor, Department of Civil Engineering, University of the District of Columbia, Washington, DC 20008, United States, E-mail: lei.wang@udc.edu (*Corresponding author)
[c]Graduate Research Assistant, Glenn Department of Civil Engineering, Clemson University, Clemson SC 29634, United States, E-mail: prahbar@g.clemson.edu
[d]Professor, Department of Civil Engineering, National Central University, Chung-Li City, Tao-Yuan 32011, Taiwan, and Glenn Department of Civil Engineering, Clemson University, Clemson, SC 29634, United States, E-mail: hsein@clemson.edu

ABSTRACT

A systematic robust design optimization methodology is presented in this study for cantilever retaining wall backfilled with shredded tire in the face of earthquake hazards. Regarding the merits of application of shredded tire backfill in seismically active areas, the uncertainties in properties of this material (e.g. friction angle and cohesion) as well as uncertainties in earthquake load (e.g. peak ground acceleration) necessitates examining the robustness of design along cost efficiency in geotechnical design procedures. The wall tip deflection was treated as the response of concern for which a response surface was developed based on the design and random (uncertain) variables. Coupling with Monte Carlo simulations, the optimization in terms of cost and standard deviation of response as a measure of robustness yielded a set of preferred designs, or Pareto front, and the final optimal design was determined via selection procedures based on knee point concept.

Keywords: Uncertainty; Design Optimization; Retaining Wall; Earthquake Hazard

1 INTRODUCTION

Recent studies show that a beneficial method for recycling waste tires is utilizing the shredded tire in geotechnical and geological engineering purposes such as embankment, road beds, soil improvement, drainage in landfill and backfill for retaining structures (Eldin and Senouci 1992; Bosscher et al. 1997; Reddy et al. 2009; Humphrey et al. 1993; Cesich 1996; Tweedie et al. 1998; Lee et al. 1999; Ravichandran and Huggins 2013; Shrestha et al. 2016; Djadouni et al. 2019). The applicability of shredded tire as an economical alternative for conventional soil backfill of retaining walls has been previously examined under dynamic loading condition compared to conventional backfill (Ravichandran and Huggins 2013; Reddy and Krishna 2015; Shrestha et al. 2016; Rahbari et al. 2016). The experimental study by Reddy and Krishna (2015) also indicated that horizontal displacements can decrease to half when adding tire chips to sand backfill. Performing finite element dynamic analysis of various cases of cantilever retaining wall, Shrestha et al. (2016) showed that using shredded tire as backfill results in considerable reduction in wall tip deflection and structural demand. It was also reported that

shredded tire backfill provides cost-efficiency in design of cantilever retaining wall, causing significant reduction in total cost of construction.

In this study, the design optimization of cantilever wall with shredded tire backfill was performed under dynamic loading condition. Generally, in the conventional design procedure the least costly design that meets the safety criteria is selected as final design. However, selecting the final design out of a great number of combinations of design parameters can be achieved through optimization methods. Various optimization approaches based on the limit equilibrium method have been used for the design of cantilever retaining wall in the past and cost (or weight) of wall was considered as the only objective of optimization (Saribas and Erbatur 1996; Ceranic et al. 2001; Yepes et al. 2008; Camp and Akin 2011). The genetic algorithm has been found to be a promising approach in design optimization when there are many design variables and multiple constraints, as in a retaining wall problem (Pei and Xia 2012, Papazafeiropoulos et al. 2013). In the above-mentioned studies, all properties of soil and loading were used as deterministic parameters. Using target reliability as safety constraint and considering uncertainties in soil properties, Babu and Basha (2008) performed a reliability based design optimization of cantilever retaining wall under static loading condition and reported a significant cost reduction in the procedure compared to conventional design optimizations. Thus, along with cost optimization, the concept of robust design was examined in the current work. Robust design is defined as the least sensitive design to the hard-to-control uncertainties identified in the system. The variation of the system response due to the high variability of hard-to-control uncertain parameters can be reduced by adjusting the easy-to-control design parameters to find the most optimal set of design parameters (Juang et al. 2013; Wang et al. 2019).

Properties of shredded tire (as a pure material or as supplementary material for soil) such as friction angle, cohesion, unit weight, permeability, and elasticity have been studied experimentally in the past for civil engineering goals. As the variability of soil parameters is required to be considered in geotechnical design (Phoon and Kalhawy 1999; Zheng et al. 2017), the use of this lightweight material as an alternative to soil backfill also involves uncertainties which may affect the system response such as wall tip deflection, shear force and bending moment introduced in the wall. Moreover, in seismic geotechnical design, uncertainties are not only limited to material properties, but also include earthquake loading properties Robust design of geotechnical structures has been proved to be beneficial in dealing with hard-to-control uncertain parameters of the geotechnical systems such as retaining walls and reducing the sensitivity of design to these parameters (Juang et al. 2012; Liu et al. 2013; Wang et al. 2013; Wang et al. 2014; Peng et al. 2017; Yu et al. 2019; Luo and Hu 2019). A reliability-based robust design optimization was performed by Juang et al. (2013) for a cantilever retaining wall under static loading condition considering uncertainties in backfill. In their study, cost and standard deviation of reliability index as the measure of robustness were considered as the objectives of optimization along with target reliability as the safety constraint. Other indices can also be used as the measure of robustness. Liu et al. (2013) performed a robust design of cantilever retaining wall using confidence level (the probability of meeting the target reliability index) as robustness measure. Moreover, standard deviation of response has been found to be an appropriate indicator of robustness so as the smaller variation in response results in a more robust design (Wang et al. 2014). Yu et al. (2019) used signal-to-noise ratio as a measure of the design robustness and performed a robust optimization of siphon drainage design considering multiple objectives including safety, cost, design robustness, and drain effectiveness.

In this study, regarding that seismic design responses are highly affected not only by the backfill properties but also by the characteristics of the seismic loading, a new procedure is presented to incorporate the variations in seismic load through robust design optimization. In this procedure dynamic finite element analysis was conducted using computed statistical properties of random variables and limiting values of design variables and a response surface was developed based on wall tip deflection results. Then, the genetic algorithm-based optimization was performed to identify the final seismic geotechnical design of cantilever retaining wall with shredded tire backfill based on performance requirement and cost limitation.

2 UNCERTAINTY IN SHREDDED TIRE PROPERTIES

The shear strength and behavior of shredded tire must be evaluated to apply the material as backfill for retaining walls. In order to identify the key properties of shredded tire as uncertain parameters (also known as random variables) in this study, a literature review was performed based on literature review on shredded tire material properties as displayed in Table 1. The material characteristics are collected in the table, and the suitability of this material for retaining wall backfill is determined based on tire size. Regarding FHWA report prepared by Balunaini et al. (2009), several researchers have investigated the properties of tire derived aggregates (TDA) for application in various geotechnical projects. In that report, the range of optimum size appropriate for backfill is mentioned as 50 mm-300 mm and the larger size tires are emphasized to be more economical in constructions.

Table 1 Properties of shredded tire

Generally, TDAs may be categorized into two types of tire chips (A) and tire shreds (B). Type A of approximately 12 mm-50 mm size and type B of 50 mm-305 mm size are considered as classifications of TDA. It should be noted that the lightweight materials of backfill are mostly taken from type B TDA and larger size tires of type A TDA. Therefore, the size range which is considered suitable for application as retaining wall backfill is assumed to be greater than 25 mm. Out of these properties, friction angle and cohesion of shredded tire backfill were considered as random variables in this study. To determine the statistical properties of these variables, the suitable data of friction angle and cohesion of shredded tire backfill was examined for fitting distribution, and the lognormal distribution was deemed to be the most appropriate one. The lognormal distribution is typically used in modeling non-negative strength properties in geotechnical and geological engineering, which is consistent with the observations of most strength testing results (Phoon and Ching 2014). The probability plots of both data for the lognormal distribution are shown in Fig. 1 and Fig. 2. The lognormal parameters of the properties were determined from the linear trendline of which slope and interception are the location (ξ) and scale (λ) parameters of the lognormally distributed variable. In the current work, the lower and upper limits of the random variables were defined as $\exp(\lambda-\xi)$ and $\exp(\lambda+\xi)$, respectively. Based on the obtained parameters, the limiting values for friction angle are 16.6° and 33.87°, and for cohesion are 4.5 kPa and 28.12 kPa.

Fig. 1 Probability plot for friction angle (φ) data of shredded tire

Fig. 2 Probability plot for cohesion (c) data of shredded tire

3 UNCERTAINTY IN EARTHQUAKE LOAD PROPERTIES

To conduct a robust geotechnical design with presence of seismic loading, identifying the

key uncertainties in strong motion parameters (such as amplitude parameters and frequency content) is of great importance (Siyahi and Arslan 2008; Huang et al. 2018). Out of these parameters, the peak ground acceleration (PGA) of the earthquake was examined in this study and the coefficient of PGA (k_{PGA}) in terms of g was considered as random variable. Assuming that this variable is lognormally distributed with unit of g, the statistical parameters can be determined using the attenuation relationship by Cornell et al. (1979) as expressed below:

$$Ln(PGA) = -0.152 + 0.859M - 1.803Ln(d_h + 25) \quad (1)$$

$$d_h = \sqrt{z^2 + d_e^{\,2}} \quad (2)$$

where M is the earthquake magnitude, d_h is the hypocentral distance (site-to-source), z is the depth of earthquake and d_e is the epicentral distance. The standard deviation of Ln(PGA) based on Cornell relationship is 0.57 which can be considered as the location parameter (ξ) of lognormal distribution. Assuming a magnitude of 7 for the earthquake and hypocentral distance of 30 km, Ln(PGA) is obtained equal to -1.365 which can be assumed as scale parameter (λ) of the lognormally distributed k_{PGA}. To this aim, a survey was conducted through more than thirty earthquakes with maximum PGA value of 0.25-0.35, as shown in Table 2. The average depth of earthquakes and average epicentral distance were obtained about 12 km and 27 km, respectively which indicates an average hypocentral distance of 30 km (Eq. 2) for an average magnitude of 7 for the surveyed earthquakes. Based on the obtained statistical parameters, the lower limit ($\exp(\lambda-\xi)$) and upper limit ($\exp(\lambda+\xi)$) for k_{PGA} were obtained equal to 0.14 and 0.45, respectively.

Table 2 Earthquakes data

4 DESIGN PARAMETERS OF THE STUDY

The key design parameters of this study, as shown in Fig. 3, are footing width, toe width, footing thickness and stem thickness, denoted as X_1, X_2, X_3 and X_4, respectively. In order to determine the limiting values of key design parameters, the stability of the retaining wall was checked using Mononobe-Okabe method (Mononobe 1924; Okabe 1924) for overturning, sliding, bearing capacity and eccentricity. Considering the limiting values of φ, c and k_{PGA}, the lower and upper limits of design variables to be implemented in defining some design cases are obtained as following:

$4.5 < X_1 < 6.1$; $3 < X_2 < 6.1$; $0.5 < X_3 < 0.87$; $0.3 < X_4 < 0.61$

As it can be observed, the range of X_2 is not consistent with typical dimension of toe in retaining walls. This long toe is due to the low unit weight of shredded tire backfill which caused difficulties in meeting eccentricity requirements. For satisfying these requirements, the toe length was increased to have a longer moment arm. Based on the obtained upper and lower limits for design variables, six different design cases were defined for conducting dynamic finite element simulations for the variations of random variables as listed in Table 2.

It should be noted that the pore water pressure is an important factor in the earthquake evaluation of retaining walls. However, in the design example used in this paper, the groundwater level is very deep and has negligible effects on the seismic performance of the retaining wall. This example is for demonstration purpose only since the focus of the paper is to

demonstrate the effectiveness of the proposed robust design method. In some cases, it is possible to encounter geological conditions with shallow groundwater table. In these scenarios, the effects of the pore water pressure can be easily integrated in the dynamic finite element modeling by considering hydro-mechanical coupling together with the proposed robust design method. Also, the hydraulic conductivity of the shredded tire is high (Huggins 2014; Shweta et al. 2016) and the effect of pore water pressure may be insignificant.

Fig. 3 Illustration of the example retaining wall (note: the slope of the line separating the in situ soil and shredded tire backfill is 60° to the horizontal)

Table 3 Design cases selected for finite element simulation

5 DYNAMIC FINITE ELEMENT ANALYSIS

Finite element method has been d

monstrated as an effective tool for modeling the static and dynamic behaviors of retaining walls (Xu et al. 2014; Huang et al. 2018; Tang et al. 2018). In this research, the dynamic finite element (FE) simulations of retaining wall-backfill-in situ soil system were conducted using PLAXIS 2D for the defined design cases. Each design case in Table 3 was analyzed for various combinations of random variables, using values of $\exp(\lambda)$, $\exp(\lambda-\xi)$ and $\exp(\lambda+\xi)$ for each random variable while keeping other variables at $\exp(\lambda)$. Thus, 7 simulations were performed for each design case and 42 simulations were carried out in total. Since the accuracy of the FE analysis results will affect the optimization results, a number of steps were taken to reduce the errors in the computed response. First, the size of the simulation domain and corresponding finite element mesh size were obtained from parametric studies following the procedure presented in Ravichandran and Huggins (2013) to ensure that the computed response, wall tip deflection in this study, is independent of mesh size and simulation domain size. In this paper, the maximum wall tip deflection computed from the deflection-time histories using the dynamic finite element analysis is considered as the system response of the retaining wall. The maximum wall tip deflection not only indicates the serviceability requirement of the retaining wall design, the excessive deflection can also signal the overall failure of the wall. If a wall satisfies the deflection requirement, it will automatically satisfy the ultimate strength requirement (against any failure mode of stability).

The parametric study resulted in the model size presented in Fig. 4 with Very Fine mesh which consists of 1800 to 2000 15-node triangular elements. In the dynamic finite element analysis, the standard fixities and the standard earthquake boundaries were applied to the model as suggested in the user manual (PLAXIS 2019). The standard fixities option fixes the vertical sides of the model domain against translation in x-direction and the base of the model domain against translation in both x and y-directions. The standard earthquake boundaries created absorbent and viscous boundary on the vertical sides, and prescribed a displacement along the bottom of the model. In addition, to accurately account the interaction between the structural components and backfill and in situ soils, interface elements were used. The properties of the interface between the tire materials and in situ soils are different from that of individual materials and also weaker than the in situ soils. The interface strength was reduced using the strength reduction factor of 0.65, which is typically used for retaining wall problems backfilled with shredded tire (Shrestha et al. 2016). Finally, the stress-strain behavior of the backfill and in situ soils were represented by the Hardening Soil (HS) model which is a nonlinear elastoplastic

model suitable for cyclic nonlinear analysis. Comparing to Mohr-Coulomb and linear elastic models, HS model is a superior model for dynamic analysis that considers soil modulus reduction and small-strain damping. The HS model input parameters, as shown in Table 4, were obtained by calibrating the HS model with Mohr-Coulomb model. Although the accuracy of the procedure followed in this study may not result in the best HS model parameters, this procedure and the model parameters were considered reasonable to demonstrate the proposed procedure.

Fig. 4 Schematic of the simulation domain and finite element mesh

Table 4 Hardening Soil input parameters of shredded tire

The computer models for each combination were analyzed by applying the first ten seconds of the El Centro 1940 earthquake acceleration-time history shown in Fig. 5(a). The PGA of the motions is approximately 0.3 g. This record is often used as the reference earthquake motion in seismic analysis of geotechnical systems. The acceleration-time history scaled to PGAs of 0.14 g, 0.25 g and 0.45 g was used as the ground motion for the finite element analyses. Sample scaled acceleration-time history for PGA = 0.14 g is shown in Fig. 5(b). The computed wall tip deflection-time histories for design cases 1 and 2 with mean φ, c and k_{PGA} are shown in Fig. 6. The wall tip deflection was computed by subtracting the wall base deflection-time history from the wall tip deflection-time history. The maximum wall tip deflections were then determined from the deflection-time histories for developing response surface. In this paper, the maximum wall tip deflection is considered as the system response of the retaining wall. The maximum wall tip deflection not only indicates the serviceability requirement of the retaining wall design, the excessive deflection can also signal the overall failure of the wall. If a wall satisfies the deflection requirement, it will automatically satisfy the ultimate strength requirement (against any failure mode of stability).

Fig. 5 El Centro 1940 earthquake acceleration-time history

Fig. 6 Wall tip deflection-time histories

6 RESPONSE SURFACE DEVELOPMENT

Using response surface method, the results obtained from finite element dynamic analysis can be utilized to establish a functional relationship between independent variables and the dependent variables (Zhang et al. 2017; Zhou and Huang 2018). Thus, in this study, a response model was developed between seven (input) variables, including three random variables (φ, c, k), four design variables (X_1, X_2, X_3, X_4), and the deflection (d) as response, by performing nonlinear regression analysis (Khuri and Mukhopadhyay 2010; Li et al. 2016). Among common models applied in response surface method, here the logarithmic regression fitted data points reasonably well and the validity of function was also evaluated. The logarithmic model adopted to express the response is as follows:

$$y = \exp\left(b_0 + \sum_{i=1}^{n} b_i Ln\left(x_i\right) \right) \tag{3}$$

where y and x denote the response and variables respectively and b_0 and b_i are the coefficients. Using this model, which brings a good interpretation of data, the response surface d shown in Eq. (4) was proposed in terms of random variables (φ, c, k_{PGA}) and design variables (X_1, X_2, X_3 and

X_4) with R-squared value of 0.941.

$$d = \exp\begin{pmatrix} 1.377 - 0.123Ln(\phi) + 0.037Ln(c) + 0.921Ln(k_{PGA}) - \\ 0.653Ln(X_1) + 0.385Ln(X_2) - 0.417Ln(X_3) - 1.03Ln(X_4) \end{pmatrix} \quad (4)$$

This relationship represents the response of the system in terms of deflection regarding the uncertain parameters and geometrical parameters. In other words, the approximate behavior of retaining wall system backfilled with lightweight material like shredded tire with specific height can be predicted considering uncertain properties and design parameters. This methodology provides an opportunity to perform the design optimization avoiding thousands of time-consuming analyses.

Moreover, the validity and performance rate of the response surface need to be evaluated. For this purpose, 20 random design sets combined with 20 random values for random variables were generated and modeled in PLAXIS 2D and the results were compared with those obtained from the response surface. Fig. 7 shows that the points are fairly adjacent to the line y=x and demonstrates a good agreement between two sets of results. However, this method of visual qualitative validation may not be adequate to guarantee the validity of response surface; additional indicators may need to be applied to quantitatively evaluate the accuracy of regression. Recommended by Moriasi et.al (2007), three quantitative statistics were computed based on FE simulation results and observation results of response surface.

Fig. 7 Graph of deflection obtained by PLAXIS and response function

Nash-Sutcliffe efficiency (NSE), percent bias (PBIAS) and ratio of the root mean square error to the standard deviation of measured data (RSR) are expressed as in Eqs. (5), (6) and (7) and categories of performance rating are listed as per Table 5:

$$NSE = 1 - \left[\frac{\sum_{i=1}^{n} \left(Y_i^{obs} - Y_i^{sim} \right)^2}{\sum_{i=1}^{n} \left(Y_i^{obs} - Y_i^{mean} \right)^2} \right] \quad (5)$$

where Y^{obs} is the observation, Y^{sim} is the simulated value and Y^{mean} is the mean of observed data. Here, the response resulted from PLAXIS 2D model and from response surface are considered as Y^{obs} and Y^{sim}, respectively.

$$PBIAS = \left[\frac{\sum_{i=1}^{n} \left(Y_i^{obs} - Y_i^{sim} \right) * 100}{\sum_{i=1}^{n} Y_i^{obs}} \right] \quad (6)$$

$$RSR = \frac{RMSE}{STDEV_{obs}} = \frac{\left[\sqrt{\sum_{i=1}^{n} \left(Y_i^{obs} - Y_i^{sim} \right)^2} \right]}{\left[\sqrt{\sum_{i=1}^{n} \left(Y_i^{obs} - Y_i^{mean} \right)^2} \right]} \quad (7)$$

Table 5 Performance ratings for recommended statistics

The computed statistics shown in Table 6 indicate that the overall validity of response surface is classified as "very good". In sum, a combination of visual technique and dimensionless statistics were utilized to validate the response surface and ensure its reliability to be used in design optimization process.

Table 6 Response surface validity performance

7 DESIGN OPTIMIZATION OF RETAINING WALL BACKFILLED WITH SHREDDED TIRE

To capture a set of preferred designs, a set of objective functions were defined to be implemented in optimization algorithm, NSGA-II (Non-dominated Sorting Genetic Algorithm) (Deb et al. 2002; Song 2011; Wang et al. 2014; Yu et al. 2019). Cost and robustness were treated as objectives in this work along with specified safety constraint. Standard deviation of response was considered as the robustness index. Minimizing the standard deviation of response corresponds to maximizing the robustness of the system and making the system less sensitive to the uncertainties involved. The objectives of design optimization of current study are described in the following.

7.1 Objective Function 1: Cost

The cost function derived for the retaining wall, as expressed Eq. (8), considers the cost of concrete used for construction of the retaining wall, the cost of earth excavation and tire shredding. The cost of concrete, excavation and tire shredding were assumed 75, 10 and 40 USD/m^3, respectively. The cost of shredded tire was estimated based on prices suggested by companies or used in relevant reports as listed in Table 7.

$$y_1 = \left(X_1X_3 + (H - X_3)X_4\right)\times\left(75\text{USD/m}^3\right) + \left(\left(\left(X_1 - X_2 - X_4\right)\times 2 + H\right)\times H/2\right)\times(10\text{USD/m}^3) + \left(\left(\left(X_1 - X_2 - X_4\right)\times 2 + H\right)\times\left(H - X_3\right)/2\right)\times(40\text{USD/m}^3) \quad (8)$$

Table 7 Shredded tire cost

7.2 Objective Function 2: Standard Deviation of Response

Standard deviation of response was computed using two methods: Monte Carlo (MC) and Taylor Series Finite Difference (TSFD). MC method involves generating random samples of the input random variables based on the lognormal distributions of the variables, computing the response for each set of variables, repeating the procedure for N number of samples and then calculating the mean value and standard deviation of response. While in TSFD method, standard deviation of response can be expressed using the relationship below (Dang et al. 2014):

$$\sigma_d = \sqrt{\left(\frac{d^+ - d^-}{2}\right)_\phi^2 + \left(\frac{d^+ - d^-}{2}\right)_c^2 + \left(\frac{d^+ - d^-}{2}\right)_{k_{PGA}}^2} \quad (9)$$

where σ_d= standard deviation of wall tip deflection, d^+= wall tip deflection corresponding to $\exp(\lambda+\xi)$ of random variable and d^-= wall tip deflection corresponding to $\exp(\lambda-\xi)$ of random variable. Therefore, using either method for computing the second objective function, we have:

$$y_2 = \sigma_d = f(X_1, X_2, X_3, X_4) \tag{10}$$

7.3 Safety Constraint

For screening designs in the design optimization process, a target reliability index (βt) equal to 3 was defined as a constraint based on serviceability limit state. This constraint prevents the designs of lower reliability from involving in the set of suitable designs. To compute the reliability index of the system, defining performance function of the system is required using the response surface and considering an allowable deflection for wall tip as below,

$$g(\theta, X) = d_{all} - d(\theta, X) \tag{11}$$

where θ and X indicate random variables and design variables, respectively, g(θ, X)= performance function, d_{all}= allowable wall tip deflection and d(θ, X)= response function. Mean value, standard deviation of performance function and reliability index were then calculated using Eqs. 12, 13 and 14, respectively.

$$\mu_g = g(\mu_\theta, X) = d_{all} - d(\mu_\phi, \mu_c, \mu_{k_{PGA}}, X_1, X_2, X_3, X_4) \tag{12}$$

$$\sigma_g = \sigma_d \tag{13}$$

$$\beta = \frac{\mu_g}{\sigma_g} \tag{14}$$

8 DESIGN OPTIMIZATION RESULTS AND DISCUSSION

The Pareto fronts established through NSGA-II consist of the computed objectives of all populations in the last generation, in which population size is equal to the number of designs dominated by other designs. Generally speaking, in NSGA-II a population of candidate solutions (design cases) of an optimization problem is developed to better solutions. The evolution, which is an iterative process, usually starts from a population of randomly generated individuals, and the whole population in each iteration is called a generation. In each iteration, after combining the populations of parents and the children, values of objective functions are evaluated, and the best individuals are sorted and selected from the current population. The new population plays the role of parents and is used for selection, crossover, and mutation to create the children population. The next generation consists of the combination of parents and children, again. Commonly, the algorithm terminates when a maximum number of generations has been produced, or the population has reached a satisfactory level (Deb et al. 2002; Yu et al. 2019).

In this study, a clear trade-off relationship between cost and the robustness index was inferred from the resulted Pareto fronts. In other words, decreasing the standard deviation of wall tip deflection which helps the system to perform in a more robust manner resulted in retaining walls of more costly designs. Using MC method in optimization, as demonstrated in Fig. 8, the computed standard deviation of deflection increased from about 0.4 cm to 0.65 cm while cost per unit length of wall decreased from 900 USD to more than 600 USD, as is shown in Fig. 9. Each point in the following set of Pareto fronts is a demonstration of a design case with its specific value of cost (per unit length) and standard deviation of wall tip deflection. Using TSFD method, another Pareto front was resulted from optimization as shown in Fig. 10. As it is observed, the range of variations of cost and standard deviation are in good agreement with the variations in

Fig. 9.

The resulted Pareto fronts can be judged by designers and the final design can be selected based on engineering preferences and available resources such as project budget. Also, a higher robustness level may be considered by designers, and a final design corresponding to that level of robustness can be determined without cost concerns. However, considering both objectives (cost and robustness level) simultaneously, the optimal final design can be determined from Pareto front using knee point concept.

Fig. 8 Flowchart of optimization using NSGA-II coupling with MC method

Fig. 9 Pareto front optimized to cost and standard deviation using MC method

Fig. 10 Pareto front optimized to cost and standard deviation using TSFD method

To determine the optimum design with respect to cost and standard deviation of wall tip deflection of the retaining wall problem, the knee point on resulted Pareto fronts were identified using two approaches; normal boundary intersection (NBI) approach and minimum distance approach. In the former method, the distances between each point on Pareto front and the boundary line, which connects the upper point and lower point of Pareto front, are computed in normalized space and the point corresponding to the maximum distance is found which is known as knee point as illustrated in Fig. 11(a). The second approach utilizes the concept of utopia point and determines the minimum distance among calculated distances between each point on Pareto front and the defined utopia point. Therefore, the knee point is the point on Pareto front corresponding to the minimum distance as illustrated in Fig. 11(b). The utopia point is originated from the concept of ideal unreal design in which all objectives are at their minimum value and the closest design point to the utopia point is considered as optimum design (Khoshnevisan et al. 2014; Luo et al. 2019). The knee point can be regarded as the most preferred design based on the gain-sacrifice relationship among designs on the Pareto Front. Above the cost level of knee point, it requires a large sacrifice in the cost efficiency (e.g., cost of the design will increase significantly) to achieve a little gain in the enhanced robustness. While below the cost level of knee point, it requires a large sacrifice in the robustness (e.g., variability of the system response will increase significantly) to achieve a little gain in the reduced cost. Using these approaches, the same knee point characteristics were obtained for both Pareto fronts presented. Moreover, the knee points identified as optimal designs resulting from optimization with methods of MC and TSFD were in good agreement as summarized in Table 8. The table represents the optimal values of design parameters of retaining wall backfilled with shredded tire with their corresponding cost and robustness measure. The results are pretty consistent with each other due to the fact that different statistical methods led us into similar design sets and it can be an evidence for appropriateness of response surface.

Fig. 11 (a) NBI approach and (b) minimum distance approach

Table 8 Knee point parameters obtained from Pareto fronts

9 CONCLUSION

The robust design optimization of retaining wall backfilled with lightweight material and subjected to seismic load was carried out through coupling of finite element dynamic analysis and bi-objective optimization. The robustness of design was satisfied by minimization of standard deviation of wall tip deflection. Along with standard deviation of response, the

expenses contributed to construction and operation of this type of wall was another objective to be minimized. On the other hand, the reliability of design was assessed and met using the concept of target reliability index and defining a performance function due to an allowable deflection. Therefore, the uncertainty in backfill parameters and in seismic loading was considered in this methodology which leads the designers to more efficient designs so as not to overdesign because of safety satisfaction, or not to underdesign because of cost concerns.

In summary, despite the advantages associated to use of shredded tire as backfill for retaining walls, the presented robust design methodology can be introduced as an efficient tool for geotechnical dynamic design of retaining structures that considers safety, robustness and cost simultaneously. Moreover, the knee point concept can be utilized to aid in selection of best design in a design pool.

ACKNOWLEDGMENTS

This research was supported by Glenn Department of Civil Engineering, Clemson University. The second author also wishes to acknowledge the support from the National Science Foundation (Award #1900445). The results and opinions expressed in this paper do not necessarily reflect the views and policies of the National Science Foundation.

REFERENCES

Ahmed, I., and Lovell, C.W. (1993). "Rubber soil as light weight geomaterials." Transportation Research Record, 61-70

Andrews, D.W., and Guay, M. A. (1996). "Tire chips in a superfund landfill cap: A case history of the first use of a tire chip drain layer." Nineteenth International Madison Waste Conference, Dept. of Engineering Professional Development, University of Wisconsin-Madison.

Babu, G. L. S. and Basha, B. M. (2008). "Optimum design of cantilever retaining walls using target reliability approach." International Journal of Geomechanics, 8, 240-252

Balunaini, U., Yoon, S., Prezzi, M. and Salgado, R. (2009). "Final report: Tire shred backfill in mechanically stabilized earth wall application." FHWA/NA/JTRP, 2008/17

Black, B.A., and Shakoor, A. (1994). "A geotechnical investigation of soil-tire mixtures for engineering applications." Proceedings of the First International Conference on Environmental Geotechnics, Bitech Publications, pp. 617-623

Bosscher, P. J., Edil, T. B. and Kuraoka, S. (1997). "Design of highway embankments using tire chips." Journal of Geotechnical and Geoenvironmental Engineering, 123(4), 295-304.

Bressette, T. (1984). "Used tire material as an alternate permeable aggregate." State of

California, Department of Transportation, Division of Engineering Services, Office of Transportation Laboratory, Sacramento, CA

Camp, C.V. and Akin, A. (2011). "Design of retaining walls using big bang–big crunch optimization." Journal of Structural Engineering, 138(3), 438-448.

Cecich, V., Gonzales, I., Hoisaeter, A., Williams, J. and Reddy, K. (1996). "Use of shredded tire as lightweight backfill material for retaining structures." Waste Management & Research, No. 14, pp. 433-451.

Ceranic, B., Fryer, C. and Baines, R.W. (2001). "An application of simulated annealing to the optimum design of reinforced concrete retaining structures." Computers & Structures, 79(17), 1569-1581.

Cornell, C. A., Banon, H., and Shakal, A. F. (1979). “Seismic motion and response prediction alternatives.” Earthquake Engineering & Structural Dynamics, 7(4), 295-315.
Cosgrove, T. A. (1995). “Interface strength between tire chips and geomembrane for use as a drainage layer in a landfill cover.” Proceedings of Geosynthetics'95, Industrial Fabrics Association, St. Paul, MN, Vol. 3, pp. 1157-1168.
Dang, H. P., Lin, H. D., and Juang, C. H. (2014). “Analyses of braced excavation considering parameter uncertainties using a finite element code.” Journal of the Chinese Institute of Engineers, 37(2), 141-151.
Djadouni, H., Trouzine, H., Correia, A. G., and da Silva Miranda, T. F. (2019). “Life cycle assessment of retaining wall backfilled with shredded tires.” The International Journal of Life Cycle Assessment, 24(3), 581-589.
Deb, K., Pratap, A. and Agarwal, S. (2002). “A fast and elitist multiobjective genetic algorithm NSGA-II.” Evolutionary Computation, 6(2), pp. 182-197.
Duffy, D. P. (1995). “Using tire chips as a leachate drainage layer,” Waste Age, Vol. 26, No. 9, pp. 113-122.
Dwyer, D.F. (2008). “Technical report: tire shred initiative: summary report.” State of New York Department of Transportation, Geotechnical Engineering Bureau
Eldin, N. N. and Senouci, A. B. (1992). “Use of scrap tires in road construction.” Journal of Construction Engineering and Management, 118(3), 561-576.
Edil, T. B. and Bosscher, P. J. (1994). “Engineering properties of tire chips and soil mixtures.” Geotechnical Testing Journal, 17(4), pp. 453-464.
Foose, G.J., Benson, C.H. and Bosscher, P.J. (1996). “Sand reinforced with shredded waste tires.” Journal of Geotechnical Engineering, 122: 760-767.
Garegrat, H. (1993). “Finite element analyses of pavements underlain by a tire chip layer and of retaining walls with tire chip backfill.” M.S. Thesis, Department of Civil Engineering, University of Maine.
Gebhardt, M. A. (1997). “Shear strength of shredded tires as applied to the design and construction of a shredded tire stream crossings.” MS Thesis, Iowa State University.
Hataf, N., and Rahimi, M.M. (2006). “Experimental investigation of bearing capacity of sand reinforced with randomly distributed tire shreds.” Construction and Building Materials, No. 20, pp. 910–916.
Head, D., Picornell, M. and Nash, P.T. (2001). “Report: El Paso embankment fill with shredded tire.” Texas Department of Transportation.
Huang, Y., Hu, H., and Xiong, M. (2018). “Probability density evolution method for seismic displacement-based assessment of earth retaining structures.” Engineering Geology, 234, 167-173.
Huggins, L. (2014). Numerical and reliability analysis of gravity cantilever retaining walls backfilled with shredded tires subjected to seismic loads. M.S. Thesis, Clemson University, Clemson, SC.
Humphrey, D.N., Sandford, T.C., Cribbs, M.M. and Manion, W.P. (1993). “Shear strength and compressibility of tire chips for use as retaining wall backfill.” Transportation Research Record, 14, 433-451.
Juang, C. H., Liu, Z. and Atamturktur, H. S. (2013). “Reliability-based robust geotechnical design of retaining walls.” Sound Geotechnical Research to Practice, pp. 514-524

Juang, C.H., Wang, L., Liu, Z., Ravichandran, N., Huang, H. and Zhang, J. (2013). "Robust geotechnical design of drilled shafts in sand: New design perspective." Journal of Geotechnical and Geoenvironmental Engineering, 139(12), 2007-2019.

Khoshnevisan, S., Gong, W., Wang, L. and Juang, C. H. (2014). "Robust design in geotechnical engineering–an update." Georisk: Assessment and Management of Risk for Engineered Systems and Geohazards, 8(4), 217-234.

Khuri, A.I., and Mukhopadhyay, S. (2010). "Response surface methodology." WIREs Computational Statistics, Vol. 2, pp. 128-149

Lee, J.H., Salgado, R., Bernal, A. and Lovell, C.W. (1999). "Shredded tires and rubber sand as lightweight backfill." Journal of Geotechnical and Geoenvironmental Engineering, 125 (2), pp. 132-141.

Li, D. Q., Zheng, D., Cao, Z. J., Tang, X. S., and Phoon, K. K. (2016). "Response surface methods for slope reliability analysis: review and comparison." Engineering Geology, 203, 3-14.

Liu, Z., Juang, C. H. and Atamturktur, S. (2013). "Confidence level-based robust design of cantilever retaining walls in sand." Computers and Geotechnics, No.52, pp. 16-27.

Luo, Z., and Hu, B. (2019). "Robust design of energy piles using a fuzzy set-based point estimate method." Cold Regions Science and Technology, 102874.

Luo, Z., Hu, B., and Pan, E. (2019). "Robust design approach for flexible pavements to minimize the influence of material property uncertainty." Construction and Building Materials, 225, 332-339.

Masad, E., Taha, R., Ho, C., and Papagiannakis, T. (1996). Engineering properties of tire/soil mixtures as a lightweight fill material. Geotechnical Testing Journal, 19(3), 297-304.

Moo-Young, H., Sellasie, K., Zeroka, D. and Sabins, G. (2003). "Physical and chemical properties of tire shreds for use in construction." Journal of Environmental Engineering, 129 (10), 921-929.

Mononobe, H. (1924). Considerations into earthquake vibrations and vibration theories. J. of the Japan Society of Civil Engrg, 10(5), 1063-1094.

Moriasi, D.N., Arnold, J.G., Van Liew, M.W., Bingner, R.L., Harmel, R.D. and Veith, T.L. (2007). "Model evaluation guidelines for systematic quantification of accuracy in watershed simulations." Transactions of the ASABE, 50(3), 885-900.

Okabe, S. (1924). General theory on earth pressure and seismic stability of retaining wall and dam. Proc. Civil Engrg. Soc., Japan, 10(6), 1277-1323.

Papazafeiropoulos , G., Plevris , V. and Papadrakakis , M. (2013). "Optimum design of cantilever walls retaining linear elastic backfill by use of genetic algorithm." COMPDYN 2013

Phoon, K. K. and Kulhawy, F. H. (1999). "Characterization of geotechnical variability." Canadian Geotechnical Journal, 36(4), 612-624.

Phoon, K. K., and Ching, J. (2014). Risk and Reliability in Geotechnical Engineering. CRC Press.

Pei, Y. and Xia, Y. (2012). "Design of reinforced cantilever retaining walls using heuristic optimization algorithms." Procedia Earth and Planetary Science, 5, 32-36.

Peng, X., Li, D. Q., Cao, Z. J., Gong, W., and Juang, C. H. (2017). "Reliability-based robust geotechnical design using Monte Carlo simulation." Bulletin of Engineering Geology and the Environment, 76(3), 1217-1227.

PLAXIS. (2019). PLAXIS 2D Reference Manual; Bentley Systems International Limited, Dublin, Ireland.

Rahbari, P., Ravichandran, N. and Juang, C. H. (2016). "Reliability-based robust geotechnical design of retaining wall backfilled with shredded tire under dynamic loads." Geotechnical and Structural Engineering Congress, Phoenix, Arizona.

Ravichandran, N. and Huggins, L. (2013). "Seismic response of gravity-cantilever retaining wall backfilled with shredded tire." Geotechnical Engineering Journal of the SEAGS & AGSSEA, Vol. 44 No. 3 14-24

RecycleNet. (2019). Retrieved from www.recyclenet.com (accessed October 1, 2019)

Reddy, S. B. and Krishna, A. M. (2015). "Recycled Tire Chips Mixed with Sand as Lightweight Backfill Material in Retaining Wall Applications: An Experimental Investigation." International Journal of Geosynthetics and Ground Engineering, 1(4), 1-11.

Reddy, K. R., Stark, T. D., and Marella, A. (2009). "Beneficial use of shredded tires as drainage material in cover systems for abandoned landfills." Practice Periodical of Hazardous, Toxic, and Radioactive Waste Management, 14(1), 47-60.

Saribas, A. and Erbatur, F. (1996). "Optimization and sensitivity of retaining structures." Journal of Geotechnical Engineering, 122(8), 649-656.

Shalaby, A. and Khan, R.A. (2005). "Design of unsurfaced roads constructed with large-sized shredded rubber tires: a case study." Resources, Conservation and Recycling, No. 44, pp. 318-332.

Shrestha, S., Ravichandran, N., Raveendra, M. and Attenhofer, J. A. (2016). "Design and analysis of retaining wall backfilled with shredded tire and subjected to earthquake shaking." Soil Dynamics and Earthquake Engineering, 90, 227-239.

Siyahi, B., and Arslan, H. (2008). Earthquake induced deformation of earth dams. Bulletin of Engineering Geology and the Environment, 67(3), 397-403.

Song, L. (2011). "NGPM - A NSGA-II program in Matlab." Aerospace Structural Dynamics Research Laboratory, College of Astronautics, Northwestern Polytechnical University, China

Tang, L., Cong, S., Xing, W., Ling, X., Geng, L., Nie, Z., and Gan, F. (2018). "Finite element analysis of lateral earth pressure on sheet pile walls." Engineering Geology, 244, 146-158.

Tatlisoz, N., Edil, T.B., and Benson, C. (1996). "Interaction between Reinforcing Geosynthetics and Soil-Tire chip mixtures." Journal of Geotechnical and Geoenvironmental Engineering, No. 124, pp. 1109-1119.

Tweedie, J. J., Humphrey, D. N. and Sandford, T. C., (1998). "Tire shreds as lightweight retaining wall backfill: active conditions." Journal of Geotechnical and Geoenvironmental Engineering, No. 124, pp. 1061-1070.

Vecoplan, LLC. (2019). Retrieved from www.vecoplanllc.com (accessed October 1, 2019)

Warith, M.A., Evgin, E. and Benson, P.A.S. (2004). "Suitability of shredded tires for use in landfill leachate collection systems." Waste Management, No. 24, pp. 967-979

Wang, L., Hwang, J. H., Juang, C. H., and Atamturktur, S. (2013). "Reliability-based design of rock slopes—a new perspective on design robustness." Engineering Geology, 154, 56-63.

Wang, L., Juang, C. H., Atamturktur, S., Gong, W., Khoshnevisan, S. and Hsieh, H. S. (2014). "Optimization of design of supported excavations in multi-layer strata." Journal of Geoengineering, Vol. 9, No. 1, pp. 1-12.

Wang, Z., Yu, Y., Sun, H., Lü, Q., and Shang, Y. (2019). "Robust optimization of the constructional time delay in the design of double-row stabilizing piles." Bulletin of Engineering Geology and the Environment, 1-15.

Wu, W., Benda, C. and Cauley, R. (1997). "Triaxial determination of shear strength of tire chips." Journal of Geotechnical and Geoenvironmental Engineering, ASCE, Vol. 123, No. 5, pp. 479-482.

Xu, Y. S., Shen, S. L., Ma, L., Sun, W. J., and Yin, Z. Y. (2014). "Evaluation of the blocking effect of retaining walls on groundwater seepage in aquifers with different insertion depths." Engineering Geology, 183, 254-264.

Yang, S., Lohnes, R.A., and Kjartanson, B.H. (2002). "Mechanical properties of shredded tires." Geotechnical Testing Journal, 25 (1), pp. 44-52

Yepes, V., Alcala, J., Perea, C. and González-Vidosa, F. (2008). "A parametric study of optimum earth-retaining walls by simulated annealing." Engineering Structures, 30(3), 821-830.

Youwai, S., and Bergado, D.T. (2003). "Strength and deformation characteristics of shredded rubber tire-sand mixtures." Canadian Geotechnical Journal, 40(2), pp. 254-264

Yu, Y., Shen, M., Sun, H., and Shang, Y. (2019). "Robust design of siphon drainage method for stabilizing rainfall-induced landslides." Engineering Geology, 249, 186-197.

Zhang, J., Wang, H., Huang, H. W., and Chen, L. H. (2017). "System reliability analysis of soil slopes stabilized with piles." Engineering Geology, 229, 45-52.

Zheng, D., Li, D. Q., Cao, Z. J., Tang, X. S., and Phoon, K. K. (2017). "An analytical method for quantifying the correlation among slope failure modes in spatially variable soils." Bulletin of Engineering Geology and the Environment, 76(4), 1343-1352.

Zhou, X. P., and Huang, X. C. (2018). "Reliability analysis of slopes using UD-based response surface methods combined with LASSO." Engineering Geology, 233, 111-123.

List of Figures

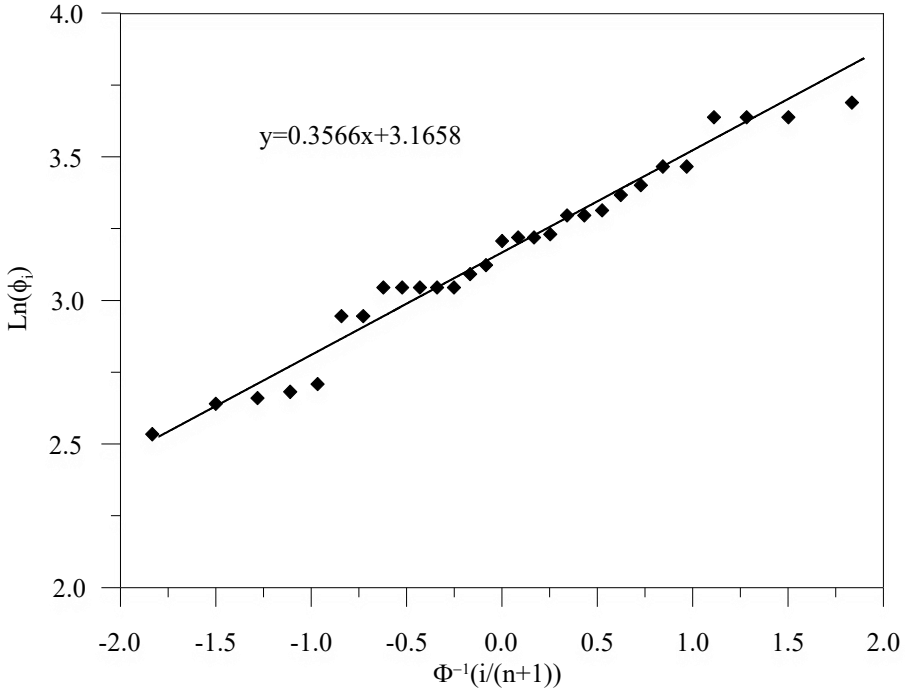

Fig. 1 Probability plot for friction angle data of shredded tire

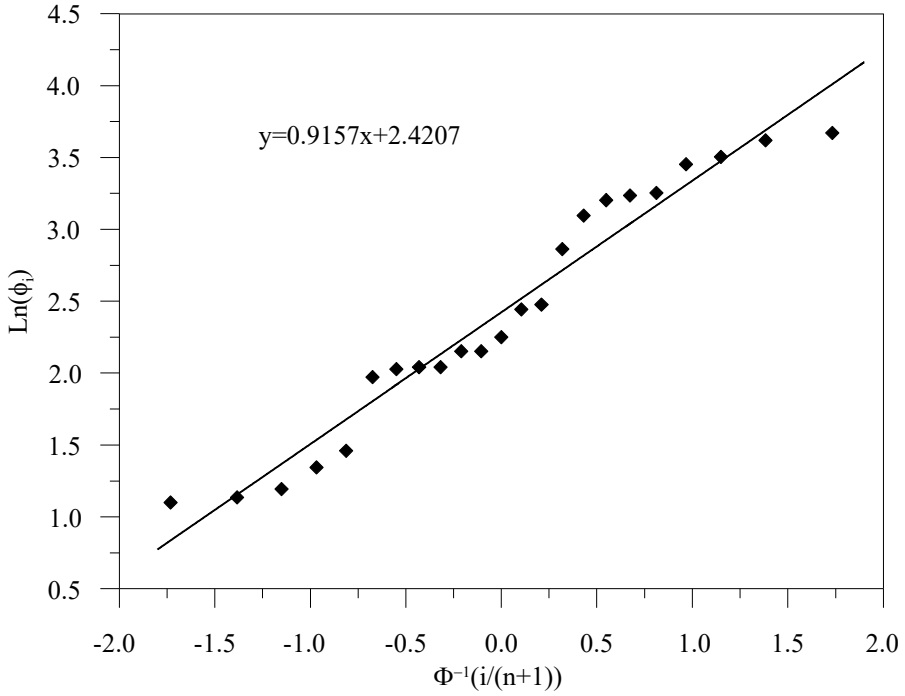

Fig. 2 Probability plot for cohesion data of shredded tire

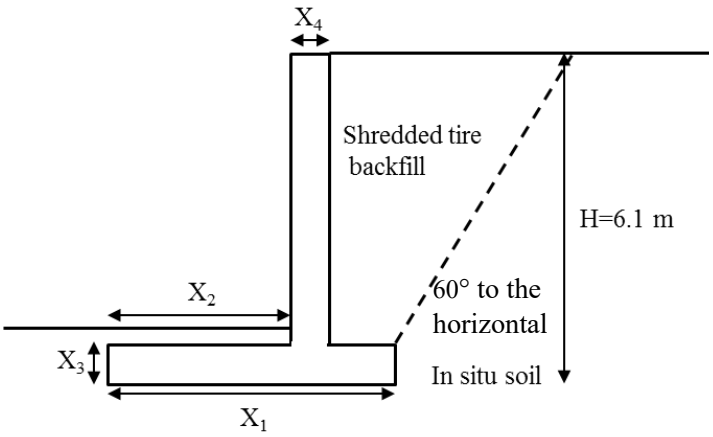

Fig. 3 Illustration of the example retaining wall (note: the slope of the line separating the in situ soil and shredded tire backfill is 60° to the horizontal)

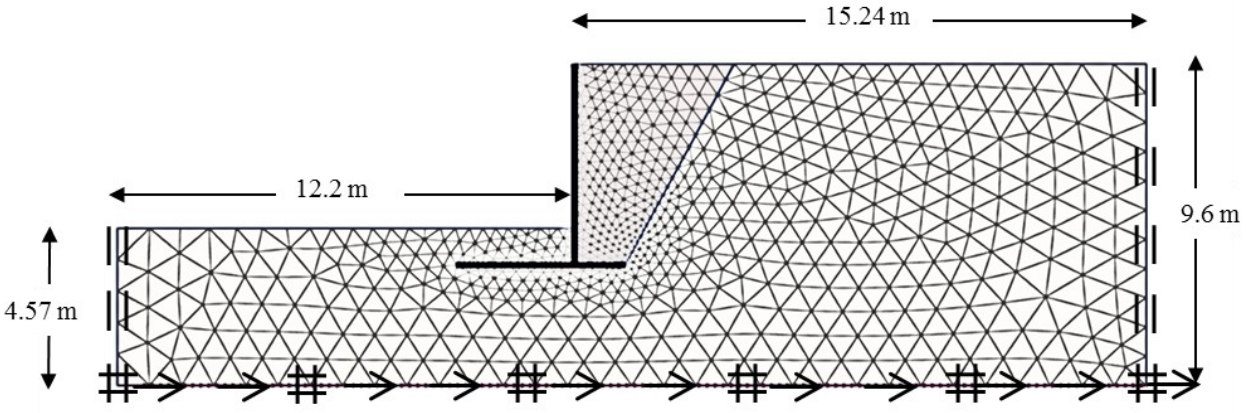

Fig. 4 Schematic of the simulation domain and finite element mesh

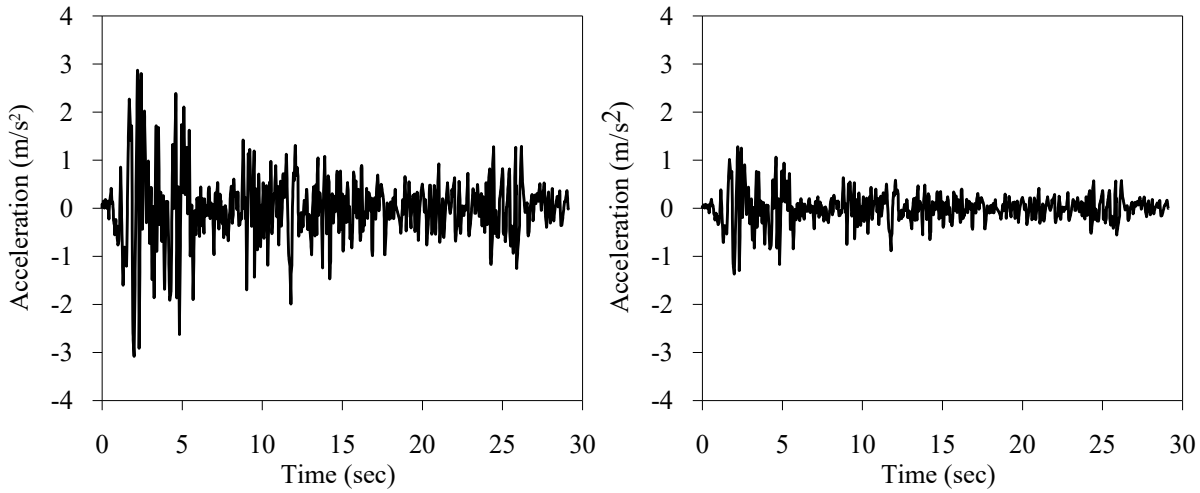

Fig. 5 El Centro 1940 earthquake acceleration-time history

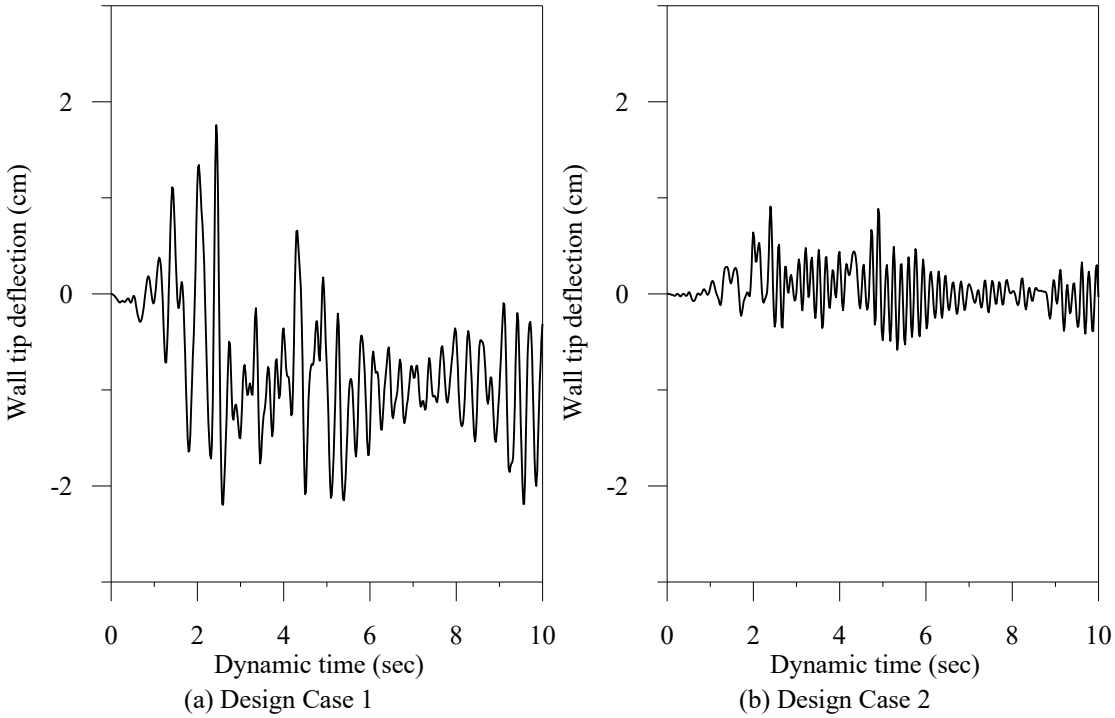

Fig. 6 Wall tip deflection-time histories

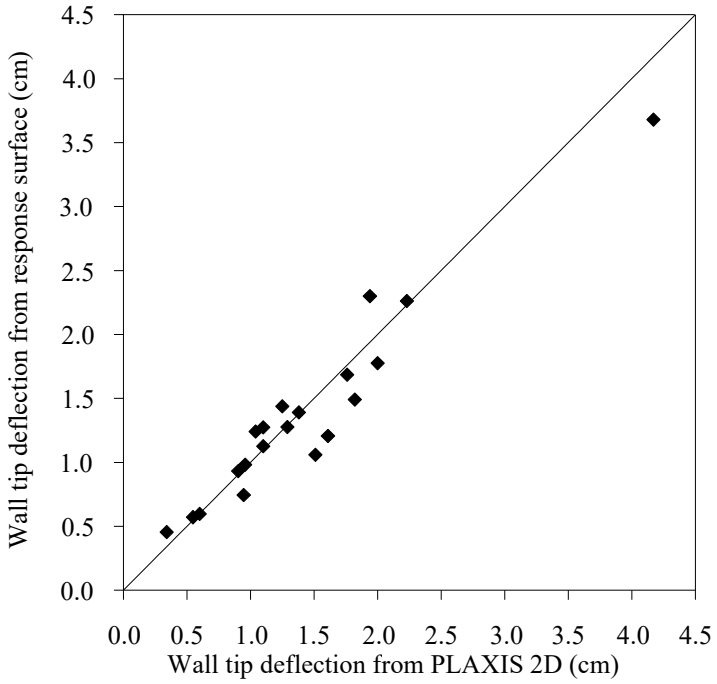

Fig. 7 Graph of comparison of wall tip deflection obtained by PLAXIS 2D and response response

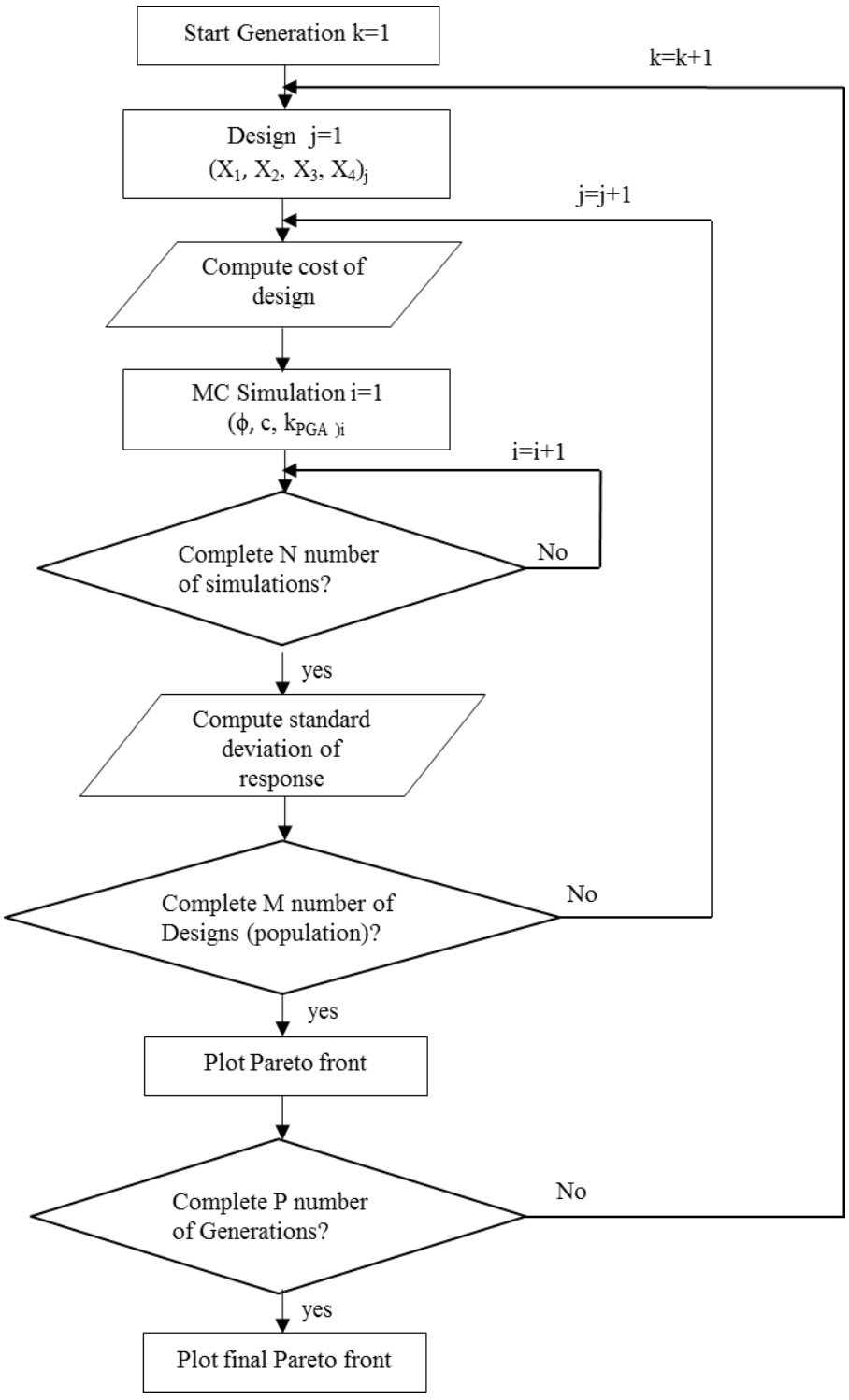

Fig. 8 Flowchart of optimization using NSGA-II coupling with MC method

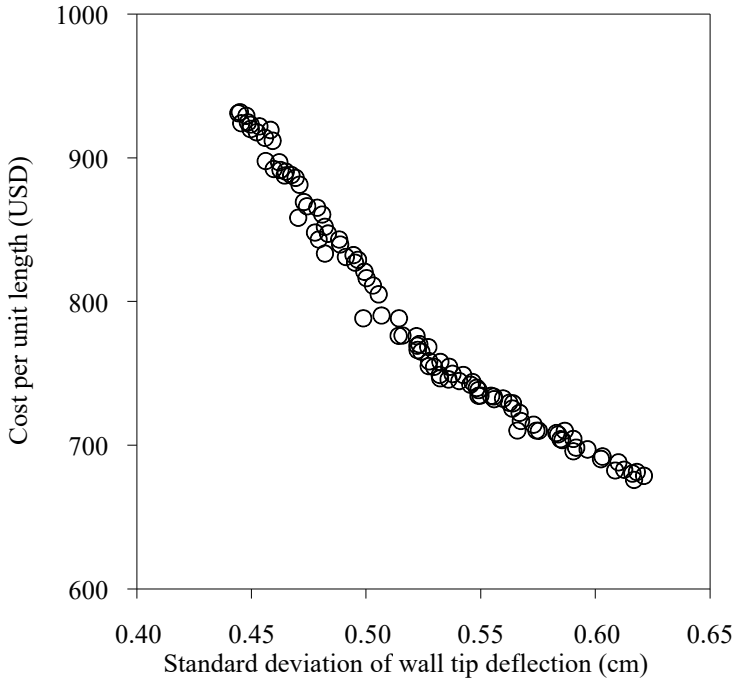

Fig. 9 Pareto front optimized to cost and standard deviation using MC method

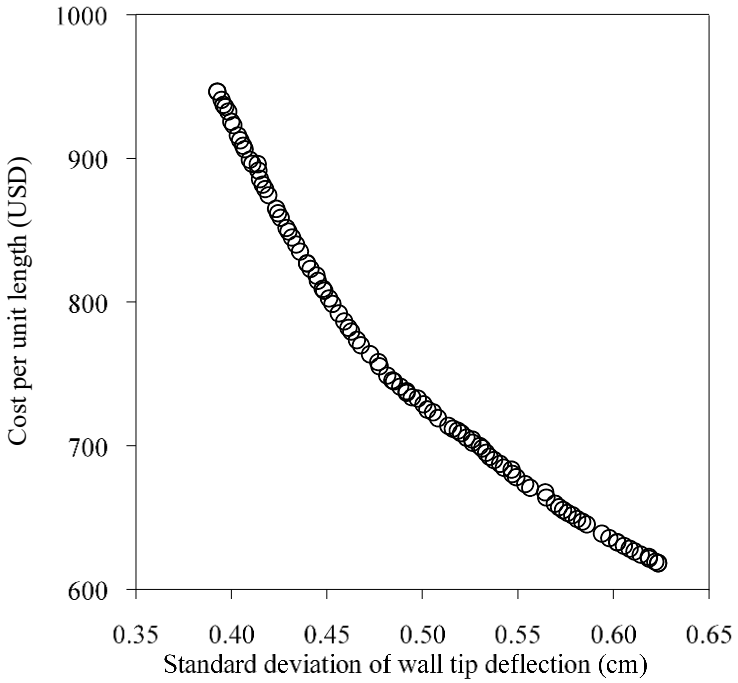

Fig. 10 Pareto front optimized to cost and standard deviation using TSFD method

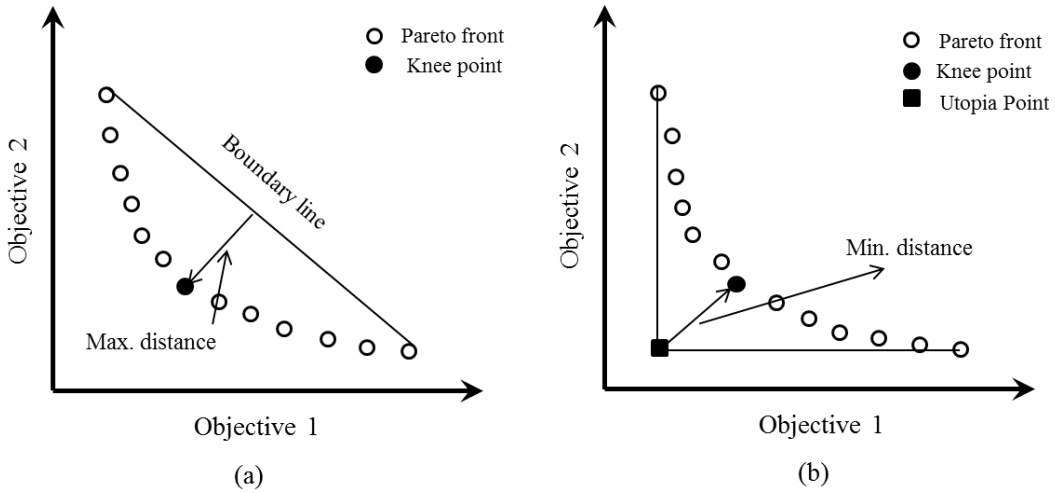

Fig. 11 (a) NBI approach and (b) minimum distance approach (modified after Khoshnevisan et al. 2014)

List of Tables

Table 1 Properties of shredded tire

Source	Tire Size (mm) /Suitability		Unit Weight (kN/m^3)	Friction Angle (deg)	Cohesion (kPa)	E (kPa)	Poisson's Ratio
Bressette (1984)	25-64	OK	4.6	21	25.85	--	--
	25-64	OK	5.96	14	31.6	--	--
Humphrey et al. (1993)	38*	OK	6.1	25	8.6	770	0.32
	51*	OK	6.3	21	7.7	1130	0.28
	76*	OK	6.1	19	11.5	1120	0.20
Gharegrat (1993)	50*	OK	6.3	21	7.6	--	--
Ahmed & Lovell (1993)	13**	N.A	6.2	11.6	22.7	--	--
	25**	OK	6.3	12.6	25.4	--	--
	25**	OK	6.4	14.6	22.1	--	--
	25**	OK	6.8	14.3	24.6	--	--
Ahmed & Lovell (1993)	13***	N.A	6.2	20.5	35.8	--	--
	25***	OK	6.3	22.7	37.3	--	--
	25***	OK	6.4	25.3	33.2	--	--
	25***	OK	6.8	24.7	39.2	--	--
Edil & Bosscher (1994)	51-76	OK	--	40	--	--	--
Black & Shakoor (1994)	Max. 1	N.A	--	30	4.79	--	--
	1-4	N.A	--	31	3.35	--	--
	4-7	N.A	--	27	6.22	--	--
Duffy (1995)	51	OK	--	27	7.18	--	--
Cosgrove (1995)	38	OK	--	38	3.3	--	--
	76	OK	--	32	4.3	--	--
Cecich et al. (1996)	12.5	N.A	5.7	27	7.04	--	--
	--	N.A	6.97	22	5.75	--	--
Andrews & Guay (1996)	25-51	OK	--	27.5	3.83	--	--
Foose et al. (1996)	50, 100, 150+	OK	5.7	30	3	--	--
Masad et al. (1996)	4.6*	N.A	6.18	6	NA	--	--
	4.6**	N.A	6.18	11	NA	--	--
	4.6***	N.A	6.18	15	NA	--	--
Wu et al. (1997)	Max. 38	OK	5.89	--	--	--	--
	Max. 19	N.A	5.69	54	0	--	--
	Max. 9.5	N.A	5.42	50.5	0	--	--
	Max. 2	N.A	5.69	45	0	--	--
Gebhardt (1997)	38-1400	OK	14.45	38	3.11	--	--
	38-1400	OK	14.45	38	0 (NA)	--	--
Tweedie et al. (1998)	Max. 38	OK	6.97	25	8.6	--	--
	Max. 76	OK	6.77	19	11.9	--	--
	Max. 76	OK	6.97	21	7.7	--	--
Tatlisoz et al.	--	N.A	5.9	30	0	--	--

(1998)							
Lee et al. (1999)	50	OK	6.3	21	17.5	3394.4	--
Yang et al. (2002)	10*	N.A	5.7	32	0	1129	0.28
	10**	N.A	5.7	11	21.6	1129	0.28
	10***	N.A	5.7	18.8	37.7	1129	0.28
Youwai & Bergado (2003)	16	N.A	7.05	30	--	--	0.33
Moo-Young et al. (2003)	50	OK	6.25	15	0.39 (NA)	--	--
	50-100	OK	7.25	32	0.37 (NA)	--	--
	100-200	OK	6.5	27	0.37 (NA)	--	--
	200-300	OK	6.25	29	0.35 (NA)	--	--
Shalaby & Khan (2005)	75	OK	6.38	22	9.5	1100	0.3
Warith et al. (2004)	75	OK	7.3	--	--	--	--
Hataf & Rahimi (2006)	--	N.A	5.8	23	0	--	--
Average input values w.r.t suitability			6.99	--	--	1502.88	0.275

[+]Direct Shear Test at 10% strain

*Triaxial Test at 10% strain, **Triaxial Test at 15% strain, ***Triaxial Test at 20% strain

Table 2 Earthquakes data

Earthquake	Year	M	PGA (g)	z (m)	d_e (m)	Earthquake	Year	M	PGA (g)	z (m)	d_e (m)
Sierra El Mayor	2010	7.2	0.27	10	22	Loma Prieta	1989	6.9	0.29	18	64
Sierra El Mayor	2010	7.2	0.27	10	34	Loma Prieta	1989	6.9	0.32	18	40
Landers	1992	7.3	0.29	1	11	Ferndale	2010	6.5	0.35	29.3	31
Landers	1992	7.3	0.3	1	24	Coalinga	1983	6.5	0.28	10	30
hector mine	1999	7.1	0.32	23.6	13	Coalinga	1983	6.5	0.27	10	38
Northridge	1994	6.7	0.34	18	3	Kyushu, Japan	2016	7	0.35	10	10
Imperial valley	1940	6.5	0.31	12	8	Kocaeli, Turkey	1999	7.6	0.32	15	5
Imperial valley	1940	6.5	0.26	12	15	El Centro	1940	7	0.3	16	13
Imperial valley	1940	6.5	0.27	12	17	Chi-Chi, Taiwan	1999	7.3	0.33	8	20
Imperial valley	1940	6.5	0.29	12	20	Chi-Chi, Taiwan	1999	7.3	0.29	8	35
Imperial valley	1940	6.5	0.26	12	30	Chi-Chi, Taiwan	1999	7.3	0.3	8	40
Petrolia	1992	7.1	0.3	15	15	Chi-Chi, Taiwan	1999	7.3	0.26	8	30
Petrolia	1992	7.1	0.32	15	25	Denali	2002	7.9	0.24	5	56
Petrolia	1992	7.1	0.26	15	30	Denali	2002	7.9	0.24	5	66
Loma Prieta	1989	6.9	0.35	18	18	Morgan hill	1984	6.2	0.31	8.4	10
Loma Prieta	1989	6.9	0.28	18	52	Morgan hill	1984	6.2	0.29	8.4	38
Average		**6.96**	**0.29**	**12.18**	**26.97**						

Table 3 Design cases selected for finite element simulation

Design variables	Design 1	Design 2	Design 3	Design 4	Design 5	Design 6
X_1 (m)	4.5	6	6	5.5	5	4.5
X_2 (m)	3	5.4	3	4	3.2	4
X_3 (m)	0.5	0.87	0.5	0.7	0.6	0.5
X_4 (m)	0.3	0.6	0.6	0.45	0.4	0.5

Table 4 Hardening Soil input parameters of shredded tire

φ′ (°)	c' (kPa)	E_{50}^{ref} (kPa)	E_{oed}^{ref} (kPa)	E_{ur}^{ref} (kPa)	m	ψ
23.71	11.25	1600	2026.84	4800	1	0
33.87	11.25	1621	2026.84	4863	1	3.87
16.6	11.25	1576	2026.84	4728	1	0
23.71	28.12	1516	2026.84	4548	1	0
23.71	4.5	1645	2026.84	4935	1	0

Note: E_{50}^{ref} is secant stiffness in standard drained triaxial test, E_{oed}^{ref} is tangent stiffness for primary oedometer loading, E_{ur}^{ref} is unloading/reloading stiffness from drained triaxial test, m is the power for stress-level dependency of stiffness, and ψ is the dilatancy angle

Table 5 Performance ratings for recommended statistics

Performance rating	**RSR**	**NSE**	**PBIAS***
Very good	0-0.5	0.75-1	<±15
Good	0.5-0.6	0.65-0.75	±15 - ±30
Satisfactory	0.6-0.7	0.5-0.65	±30 - ±55
Unsatisfactory	>0.7	<0.5	> ±55

*Ranges were problem-dependent and the average one is considered here.

Table 6 Response surface validity performance

Statistics	Value	Performance
RSR	0.29	Very Good
NSE	0.92	Very Good
PBIAS	3.58	Very Good

Table 7 Shredded tire cost

Source	Size	Price (USD)	(USD/m3)
recycle.net (accessed April 18, 2019)	mix	80 /ton	63.0
	mix	45/ton	35.4
	<3"	40/ton	31.5
	mix	64/ton	50.3
	<4"	40/ton	31.5
	<2"	28/ton	22.0
vecoplanllc.com (accessed April 18, 2019)	2"	25-50 /ton	20-40
Head et al. (2001)	--	--	12
Dwyer (2008)	--	--	80-90
Average ~	--	--	**40**

Table 8 Knee point parameters obtained from Pareto fronts

Method	Cost (USD)	Standard Deviation (cm)	X_1 (m)	X_2 (m)	X_3 (m)	X_4 (m)
MC	788	0.49	4.74	3	0.87	0.6
TSFD	749	0.48	4.5	3	0.84	0.6